Supplemental Figure 1

A

```
hSSB1 (Richard et al., 2008) ................MTTETFVKDIKPGLKNLNLIFIVLETGRVTKTKDGHEVRTCKVADKTGSINISVWDDVGNLIQPGDIIRLTKG
     human OBFC2B (ensemble) ................MTTETFVKDIKPGLKNLNLIFIVLETGRVTKTKDGHEVRTCKVADKTGSINISVWDDVGNLIQPGDIIRLTKG
        mouse Obfc2b (212aa) ................MTTETFVKDIKPGLKNLNLIFIVLETGRVTKTKDGHEVRTCKVADKTGSINISVWDDVGNLIQPGDIIRLTKG
        mouse Obfc2b (228aa) MRVQEDLPTGCHGSGSMTTETFVKDIKPGLKNLNLIFIVLETGRVTKTKDGHEVRTCKVADKTGSINISVWDDVGNLIQPGDIIRLTKG

hSSB1 (Richard et al., 2008)
     human OBFC2B (ensemble) YASVFKGCLTLYTGRGGDLQKIGEFCMVYSEVPNFSEPNPEYSTQQAPNKAVQN-DSNPSASQPTTGPSAASPASENQNGNGLSAPPGP
        mouse Obfc2b (212aa) YASVFKGCLTLYTGRGGDLQKIGEFCMVYSEVPNFSEPNPEYSTQQAPNKAVQN-DSNPSASQPTTGPSAASPASENQNGNGLSAPPGP
        mouse Obfc2b (228aa) YASVFKGCLTLYTGRGGDLQKIGEFCMVYSEVPNFSEPNPEYNTQQAPNKSVQNNDNSPTAPQATTGPPAASPASENQNGNGLSTQLGP
hSSB1 (Richard et al., 2008) YASVFKGCLTLYTGRGGDLQKIGEFCMVYSEVPNFSEPNPEYNTQQAPNKSVQNNDNSPTAPQATTGPPAASPASENQNGNGLSTQLGP
     human OBFC2B (ensemble)
        mouse Obfc2b (212aa) GGGPHPPHTPSHPPSTRITRSQPNHTPAGPPGPSSNPVSNGKETRRSSKR Chromosome 12; 13q
        mouse Obfc2b (228aa) GGGPHPPHTPSHPPSTRITRSQPNHTPAGPPGPSSNPVSNGKETRRSSKR Chromosome 12; 13q
                             VGGPHPSHTPSHPPSTRITRSQPNHTPSGPPGPSSNPVSNGKETRRSSKR Chromosome 10; D3
                             VGGPHPSHTPSHPPSTRITRSQPNHTPSGPPGPSSNPVSNGKETRRSSKR Chromosome 10; D3


        mouse Obfc2b (212aa) ................MTTETFVKDIKPGLKNLNLIFIVLETGRVTKTKDGHEVRTCKVADKTGSINISVWDDVGNLIQPGDIIRLTKG
        mouse Obfc2b (228aa) MRVQEDLPTGCHGSGSMTTETFVKDIKPGLKNLNLIFIVLETGRVTKTKDGHEVRTCKVADKTGSINISVWDDVGNLIQPGDIIRLTKG
                mouse Obfc2a ..........  MHGVNDPPLFIKDIKAGLKNLNVVFIVLEIGRVTKTKDGHEVRSCKVADRTGSITISVWDEIGGLIQTGDIIRLTRG

        mouse Obfc2b (212aa)
        mouse Obfc2b (228aa) YASVFKGCLTLYTGRGGDLQKIGEFCMVYSEVPNFSEPNPEYNTQQAPNKSVQNNDNSPTAPQATTGPPAASPASENQNGNGLSTQLGP
                mouse Obfc2a YASVFKGCLTLYTGRGGDLQKIGEFCMVYSEVPNFSEPNPEYNTQQAPNKSVQNNDNSPTAPQATTGPPAASPASENQNGNGLSTQLGP
                             YASMWKGCLTLYTGRGGELQKIGEFCMVYSEVPNFSEPNPDYRGQQ--NRGVQNEQKDKLS--TNTFGPVGNGDQTGPESRGYHLPYGR
        mouse Obfc2b (212aa)
        mouse Obfc2b (228aa) VGGPHPSHTPSHPPSTRITRSQPNHTPSGPPGPSSNPVSNGKETRRSSKR Chromosome 10; D3
                mouse Obfc2a VGGPHPSHTPSHPPSTRITRSQPNHTPSGPPGPSSNPVSNGKETRRSSKR Chromosome 10; D3
                             SNGPGPI-SPQLPG-----------TPSSQTVRTT--ISNARDPRRAFKR Chromosome 1; C1.1
```

B

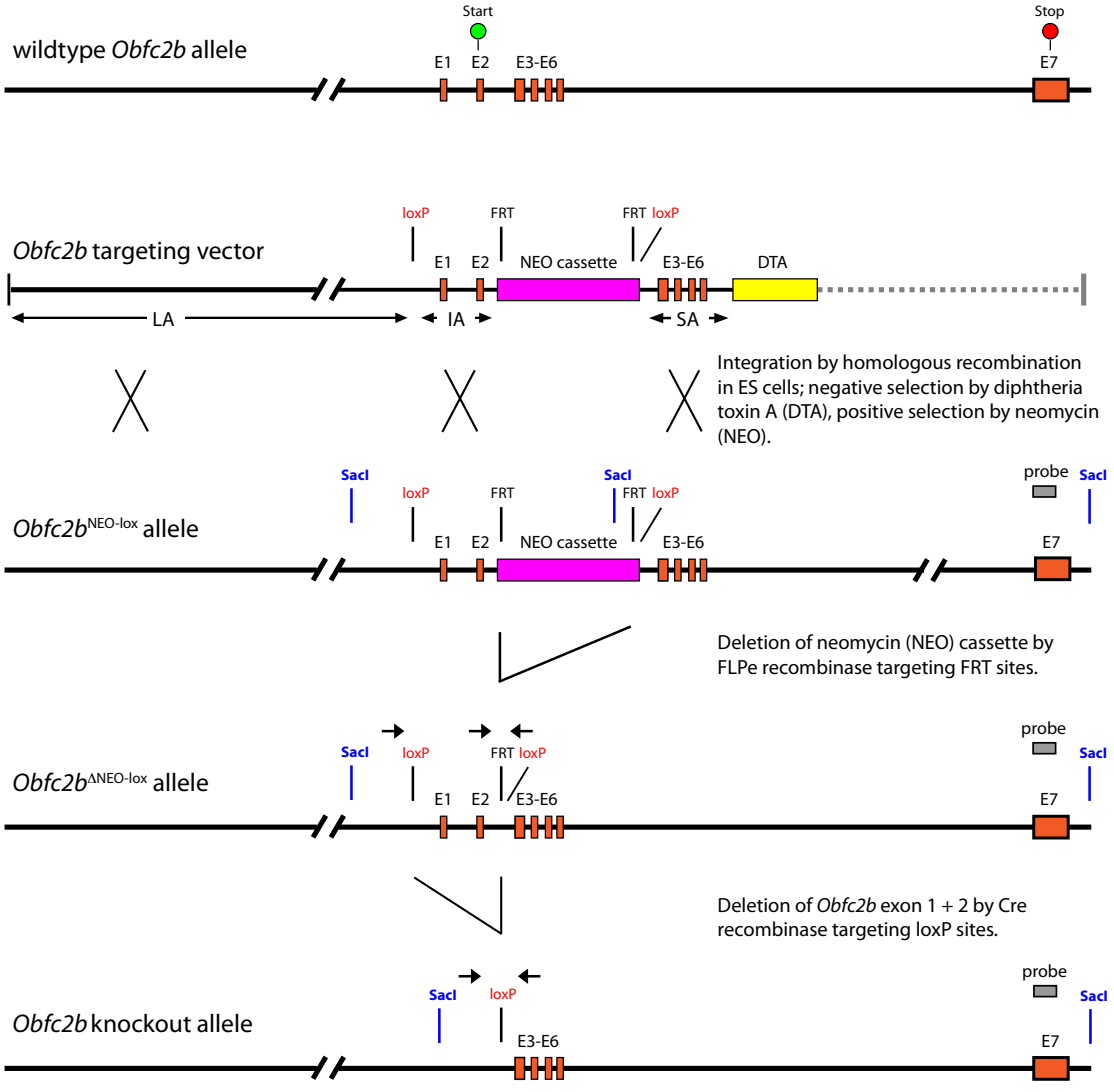

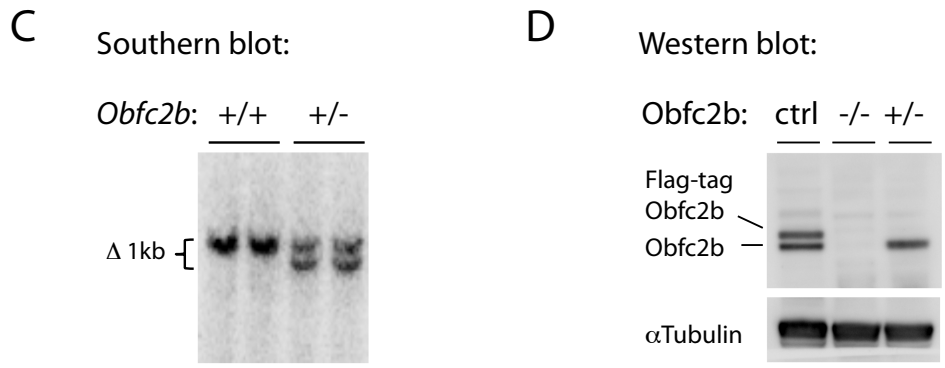

Supplemental Figure 1: Gene targeting strategy to generate conditional knockout mice for the mouse *hSsb1* orthologue *Obfc2b*.

(A) Alignment of the amino acid sequences of human hSSB1 (Richard et al., 2008), human OBFC2B (ensemble) and mouse Obfc2b (ensemble; upper panel). (Lower panel) Alignment of mouse Obfc2b (hSsb1) and Obfc2a (hSsb2) amino acid sequences (ensemble). (B) Gene targeting strategy showing the wildtype *Obfc2b* allele, the *Obfc2b* targeting vector, the targeted *Obfc2b*$^{NEO\text{-}lox}$ allele carrying the neomycin cassette, the targeted allele after excision of the neomycin cassette by FRT site specific recombination using FLPe mice (*Obfc2b*$^{\Delta NEO\text{-}lox}$), and the targeted "knockout" allele after excision of Exon 1 and 2 of *Obfc2b* by loxP site specific recombination using *EIIA*^{Cre} mice. Diphtheria toxin A (DTA) was used for negative selection during ES cell targeting, neomycin was used for positive selection. Genomic sequences of the *Obfc2b* gene for the generation of the targeting vector were amplified using the following primers: 5′-CTCGAGCCCGGCAGGTAAAGGTAAAT-3′ and 5′-ACCGGTGCTAGGTTAATTAAAATATTATGGAATGCAGCAGGAAAAC-3′ (long arm, LA), 5′-TTAATTAAATAACTTCGTATAATGTATGCTATACGAAGTTATCGCCCTTGGACCTTTTTTCC-3′ and 5′-ACCGGTGGCCGGCCTTTTATACCTGTCAGCAGCTCCC-3′ (intermediate arm, IA), 5′-TTAATTAATAGGTAAAACTAAATGGCCTGATG-3′ and 5′-GCGGCCGCATCCTGTTTGGCACACCTGG-3′ (short arm, SA). For genotyping of *Obfc2b* wildtype, knockout and *Obfc2b*$^{NEO\text{-}lox}$ alleles by Southern blot, genomic DNA was digested by SacI and blotted as previously described (Robbiani et al., 2008). The probe for Southern blot was generated using 5′-CGAGAACCAGAACGGAAATGG-3′ as forward and 5′-GGTGGAAGGAAGGAGAGACTCATC-3′ as reverse primer. Location of the probe used and the SacI recognition sites is indicated in A. For genotyping by PCR, wildtype, knockout and *Obfc2b*^{lox} alleles were amplified using the following primers and conditions: 5′-GGGAGCTGCTGACAGGTATAAAA-3′ and 5′-GATAGTGGTGATGGTGAGAGTCCG-3′ for amplification of wildtype (214 nt) and floxed allele (322 nt), and 5′-GATAGTGGTGATGGTGAGAGTCCG-3′ and 5′-GGCTTGCTTTTTATGTTCCG-3′ for amplification of the knockout allele (639 nt, 35 cycles using 56.5 C annealing temperature and 45 s extension time). Location of primers used for genotyping PCRs is indicated by arrows. (C) Presence of the *Obfc2b* knockout allele was confirmed by Southern blot on tail genomic DNA. (D) Loss of Obfc2b protein was verified by Western blot on lysates from *CD19*^{Cre}; *Obfc2b*$^{lox/-}$ B cells. Lysates of BOSC23 cells expressing Flag-tag Obfc2b protein were used as positive controls.

A

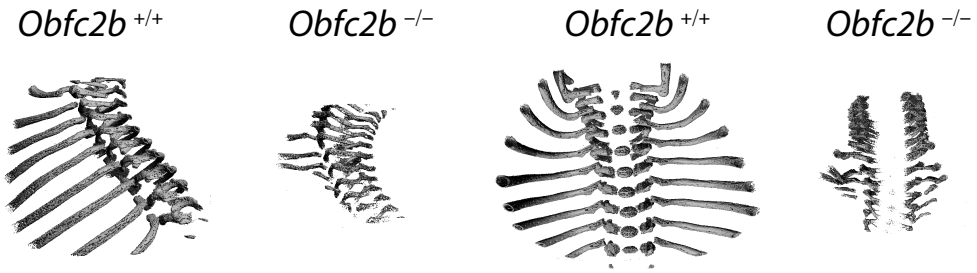

B

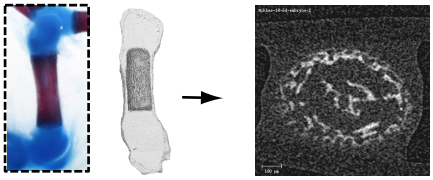

C

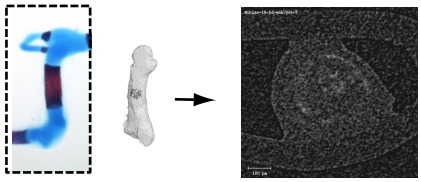

D

Genotype	Scan	Total Volume	Bone Volume	Bone/Total Volume	Mineral Density
Obfc2b$^{+/+}$	femur	0.9215	0.0943	0.1024	606.3
Obfc2b$^{+/+}$	femur	0.8695	0.0658	0.0757	517.8
Obfc2b$^{+/-}$	femur	0.8054	0.0505	0.0627	463.5
Obfc2b$^{-/-}$	femur	0.1704	0.0001	0.0008	407.0
Obfc2b$^{-/-}$	femur	0.1183	0.0000	0.0001	-140.2
Obfc2b$^{-/-}$	femur	0.1357	0.0053	0.0391	555.9

Supplemental Figure 2: MicroCT analysis of skeletal defects in *Obfc2b*$^{-/-}$ embryos.
(A) Rib cage regions from whole embryos (P0) were scanned by micro-computer tomography (MicroCT). (B/C) Femurs from skeletal preparations of E18.5 embryos (left) are screened by MicroCT and shown as three-dimensional (middle) and two-dimensional images (right). The latter are cross-sections of the mineralized fraction. (D) Values of MicroCT analysis of femurs from two *Obfc2b* wildtype (+/+), one heterozygous (+/-) and three knockout (-/-) embryos as shown in B/C.

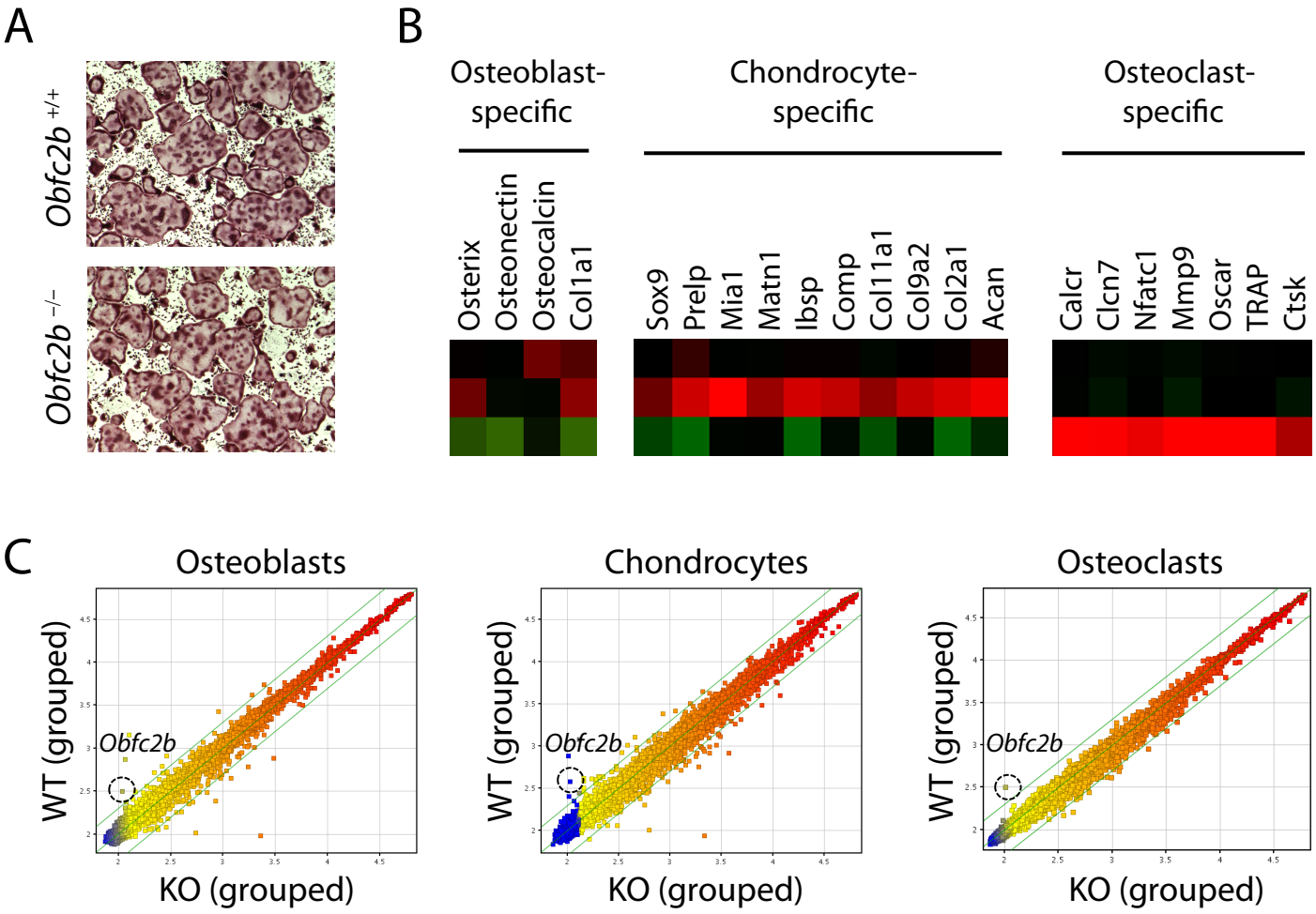

Supplemental Figure 3: Loss of *Obfc2b* does not result in significant changes in isolated chondrocytes, osteoblasts and osteoclasts.

(A) Tartrate-resistant Acidic Phosphatase (TRAP) staining of *Obfc2b*$^{+/+}$ and *Obfc2b*$^{-/-}$ bone marrow cells after 5 days in cell culture with 30ng/ml murine M-CSF and 40ng/ml RANK-L. (B, C) Gene array analysis (Illumina MouseRef-8 v2.0 Expression BeadChip) of chondrocytes isolated from the sternum, osteoblast isolated from the calvaria of the skull, and osteoclast induced by 5 days of stimulation by RANK-L and M-CSF as described in (A). Shown are average values of two independent experiments. (B) The expression values of genes specific for osteoclast, chondrocyte and osteoclast lineages, respectively, are shown by heat map representation for *Obfc2b*$^{+/+}$ cells. (C) Dot plot diagrams representing gene array results by comparing the expression values of *Obfc2b*$^{+/+}$ and *Obfc2b*$^{-/-}$ cells. Note that the only significant differences relate to *Obfc2b* or genes encoded by X- and Y-chromosomes.

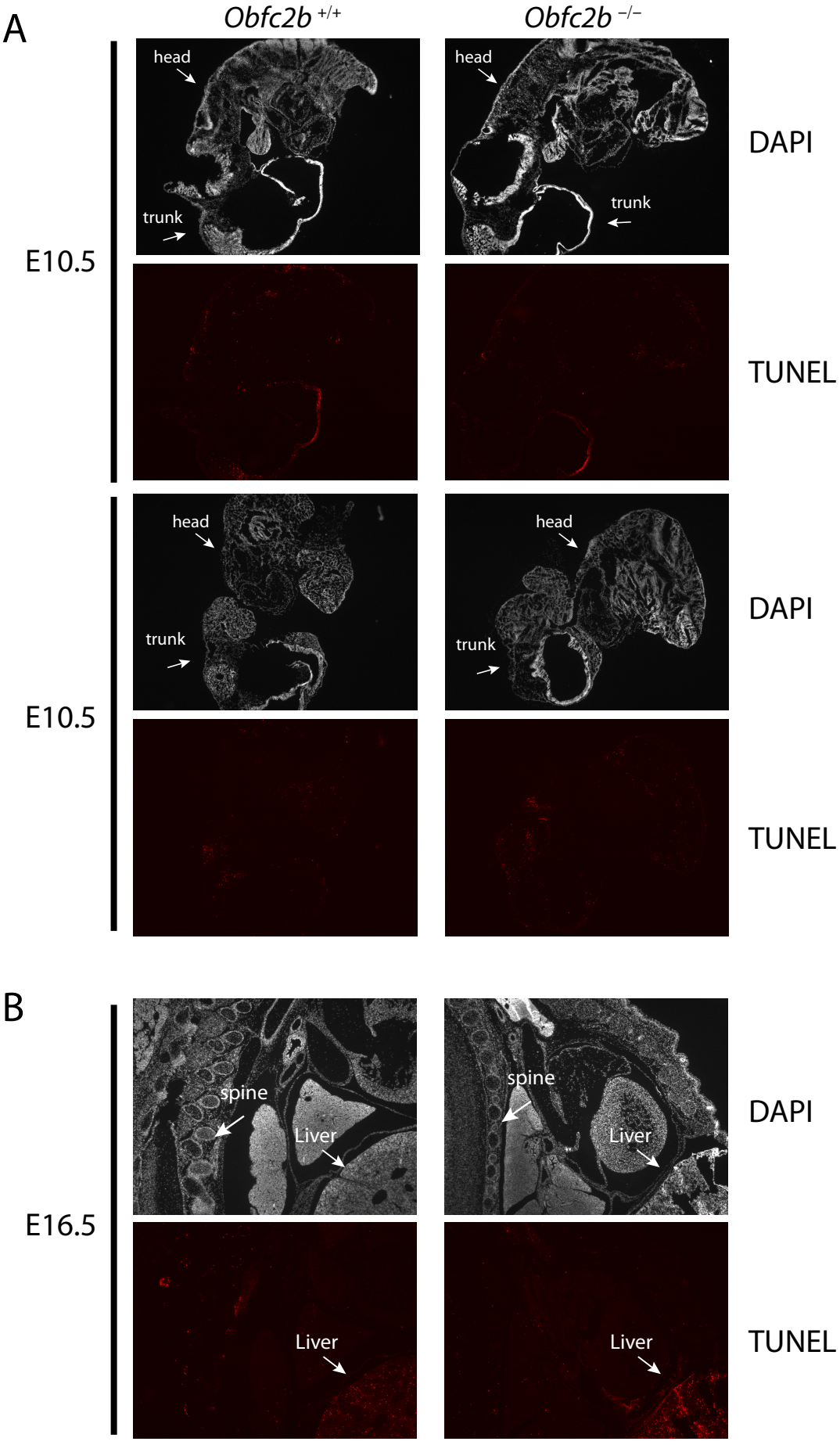
A
Obfc2b +/+
Obfc2b −/−
head
trunk
DAPI
TUNEL
E10.5
B
spine
Liver
E16.5

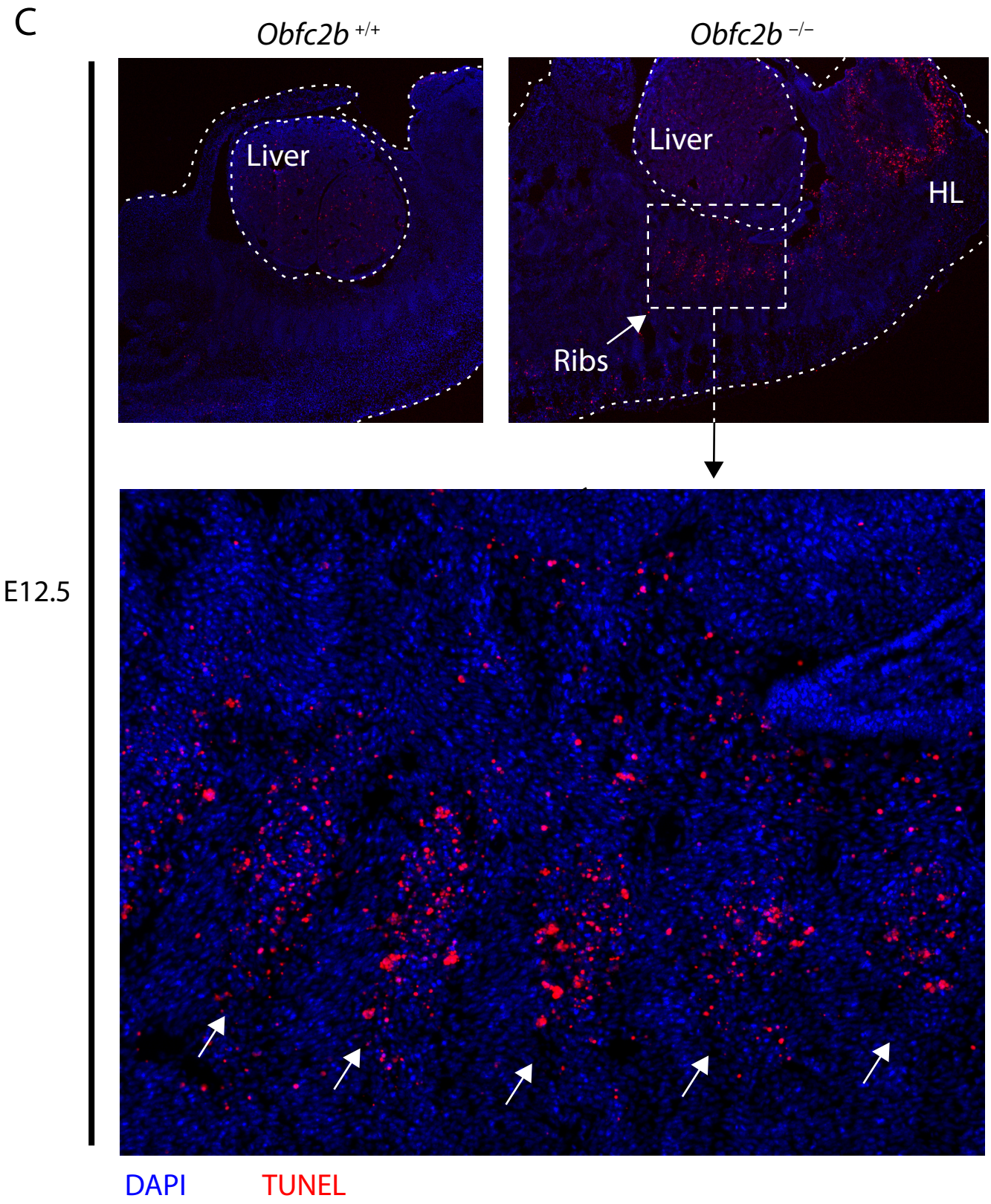

Supplemental Figure 4: TUNEL analysis of *Obfc2b*$^{+/+}$ and *Obfc2b*$^{-/-}$ embryos from E10.5 and E16.5.
(A/B) Sections from E10.5 (A) and E16.5 (B) embryos were stained with DAPI and by TUNEL. Representative slides are shown. For each time point two *Obfc2b*$^{+/+}$ and two *Obfc2b*$^{-/-}$ embryos were analyzed. (C) Representative slides of DAPI (blue) and TUNEL (red) stained tissue sections from E12.5 embryos as shown in Figure 3 (upper panel). Enlarged image of the area of developing ribs in *Obfc2b*$^{-/-}$ embryos showing extensive apoptosis by TUNEL staining is shown seperately (lower panel).

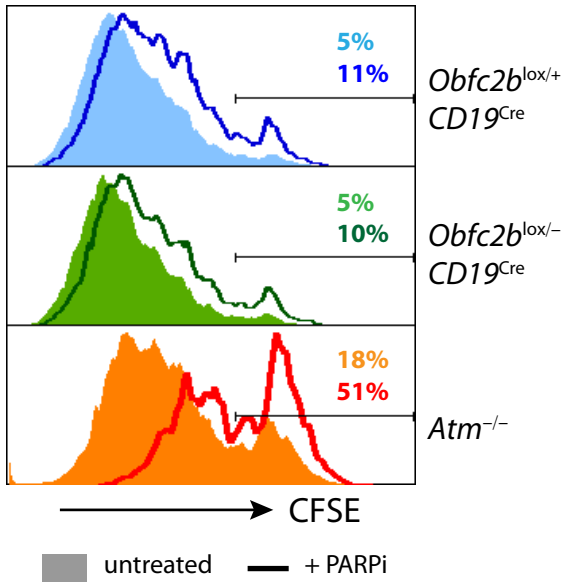

Supplemental Figure 5: PARPi sensitivity analysis
Sensitivity to inhibitor of Poly-ADP-Ribose-Polymerase (PARPi): B cells were labeled with carboxyfluorescein succinimidyl ester (CFSE) to visualize proliferation and kept for 4 days in culture with LPS and IL4, and with or without 1μM Ku58948 (PARPi). For quantification of cells with delayed proliferation (CFSE-positive), a gate for untreated control cells (*Obfc2b*$^{+/+}$;*CD19*$^{Cre/+}$ or *Obfc2b*$^{lox/+}$;*CD19*$^{Cre/+}$) was set to contain 5% of CFSE-positive cells for each individual experiment. The percentage was then compared to the percentage of cells within this gate for all other conditions.

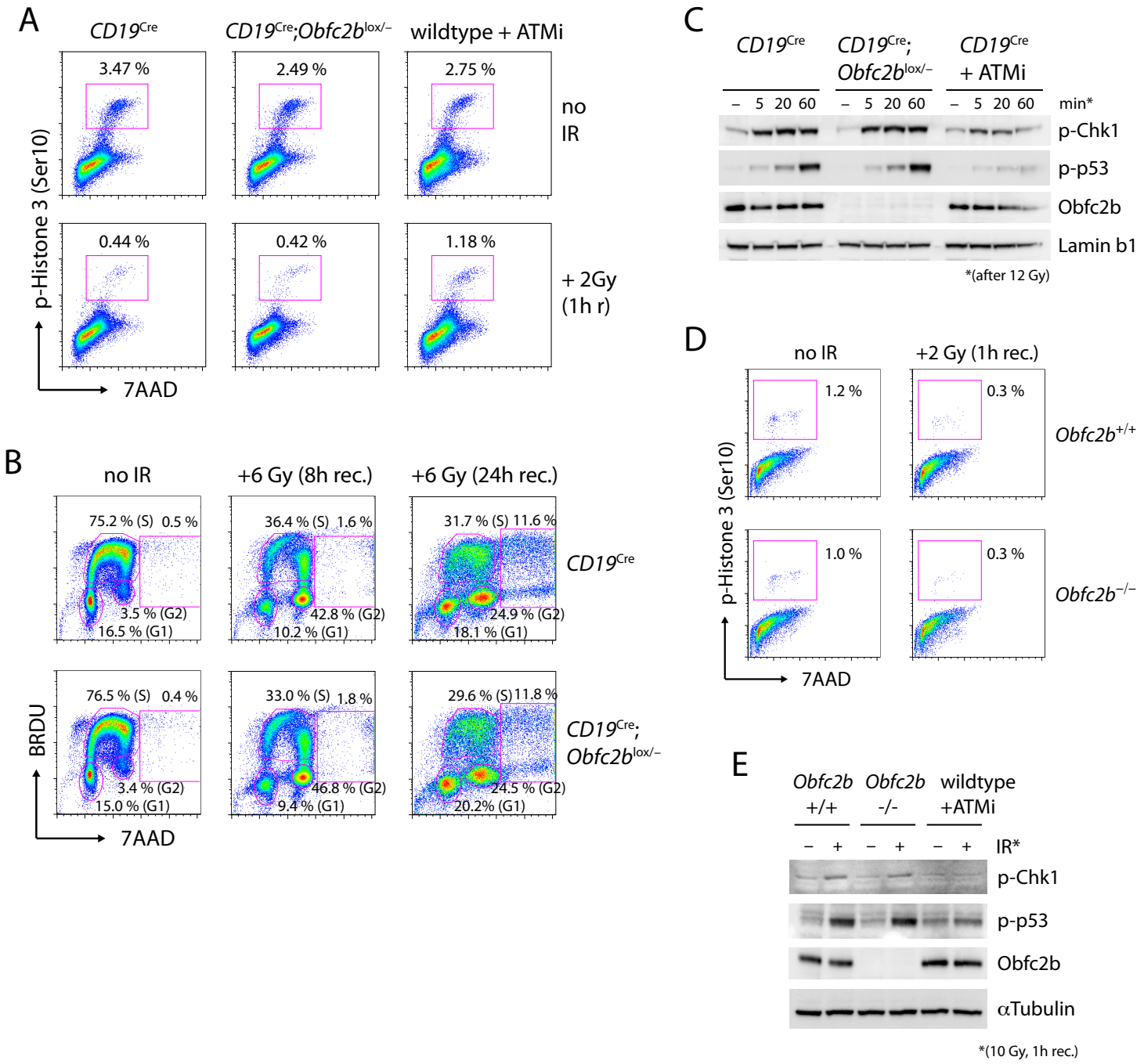

Supplemental Figure 6: PARPi sensitivity and cell cycle analysis

(A) Normal G2/M checkpoint in *Obfc2b*$^{-/-}$ B cells. Proliferating B cells from wildtype (*CD19*$^{Cre/+}$;Obfc2b$^{+/+}$) and conditional knockout (*CD19*$^{Cre/+}$;*Obfc2b*$^{lox/-}$) mice were analyzed for Histone 3 (Ser10) phosphorylation before and after irradiation (2Gy, 1 hour recovery). 7AAD was used to stain DNA content. As a control, wildtype (*CD19*$^{Cre/+}$;*Obfc2b*$^{+/+}$) B cells were treated with 2.5μM Ku55933 (ATMi). Numbers indicate the percentage of cells with Histone 3 phosphorylation. (B) Normal G1/S checkpoint in *Obfc2b*$^{-/-}$ B cells. Proliferating B cells from wildtype (*CD19*$^{Cre/+}$;*Obfc2b*$^{+/+}$) and conditional knockout (*CD19*$^{Cre/+}$;*Obfc2b*$^{lox/-}$) mice were pulsed with BrdU and subjected to cell cycle analysis. Cells were either mock treated (left) or irradiated with 6 Gy, and allowed to recover for 8 (middle) or 24 hours (right). 7AAD was used to stain DNA content. Numbers indicate the percentage of cells in G1-, S- and G2 phase of the cell cycle; or the percentage of cells with >4N. (C) Western blot analysis of irradiation induced phosphorylation of Chk1 (Ser317) and p53 (Ser15) at different time points post IR (12 Gy) as indicated. Proliferating B cells from wildtype (*CD19*$^{Cre/+}$;*Obfc2b*$^{+/+}$) and conditional knockout (*CD19*$^{Cre/+}$;*Obfc2b*$^{lox/-}$) mice were used. Wildtype (*CD19*$^{Cre/+}$;*Obfc2b*$^{+/+}$) B cells treated with 2.5μM Ku55933 (ATMi) were used as a control. (D) Normal G2/M checkpoint in Obfc2b$^{-/-}$ MEFs. Primary Obfc2b$^{+/+}$ and Obfc2b$^{-/-}$ MEFs were analyzed for Histone 3 (Ser10) phosphorylation before and after irradiation (2Gy, 1 hour recovery). 7AAD was used to stain DNA content. (E) Normal IR-induced phosphorylations in Obfc2b$^{-/-}$ MEFs. Western blot for phosphorylated Chk1 (Ser317), p53 (Ser15), and for Obfc2b and αTubulin on lysates from primary Obfc2b$^{+/+}$ and Obfc2b$^{-/-}$ MEFs irradiated as indicated. As a control, wildtype MEFs have been treated with 2.5 μM Ku55933 (ATMi) one hour before irradiation.

Supplemental Figure 7

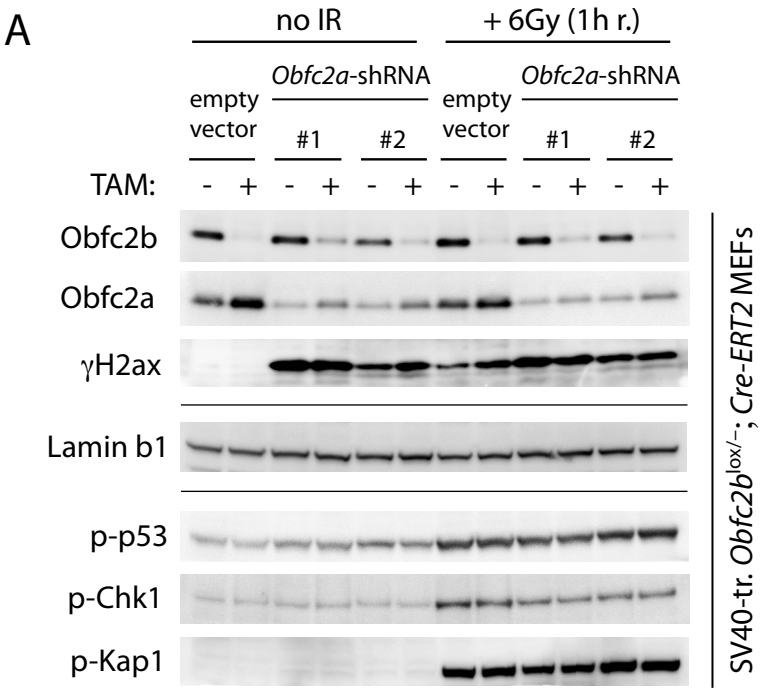

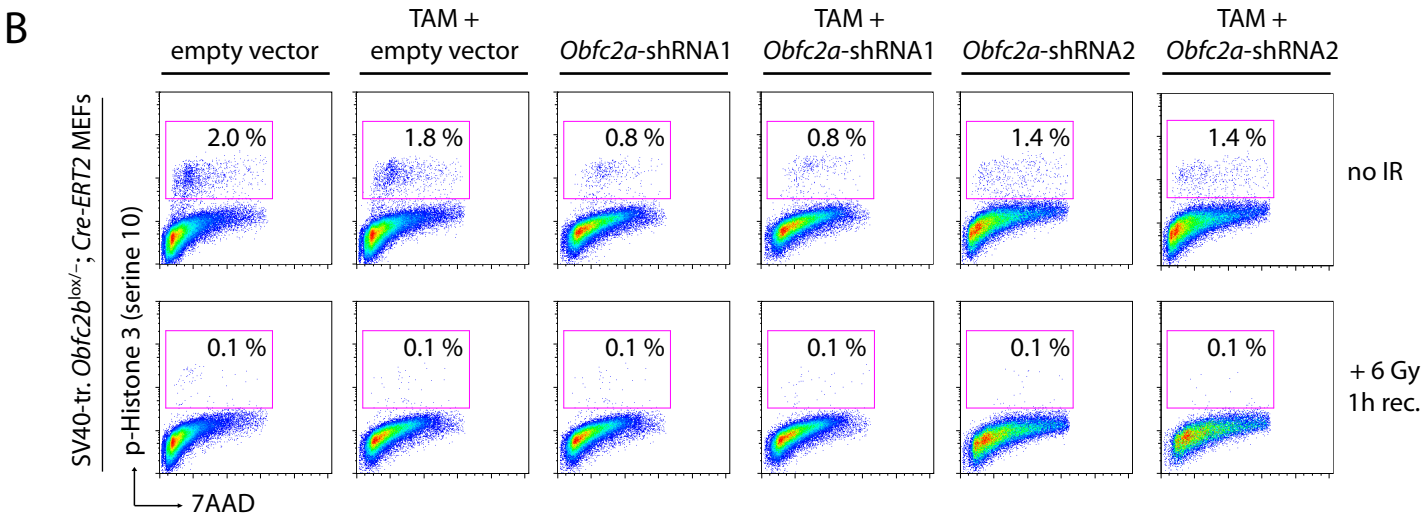

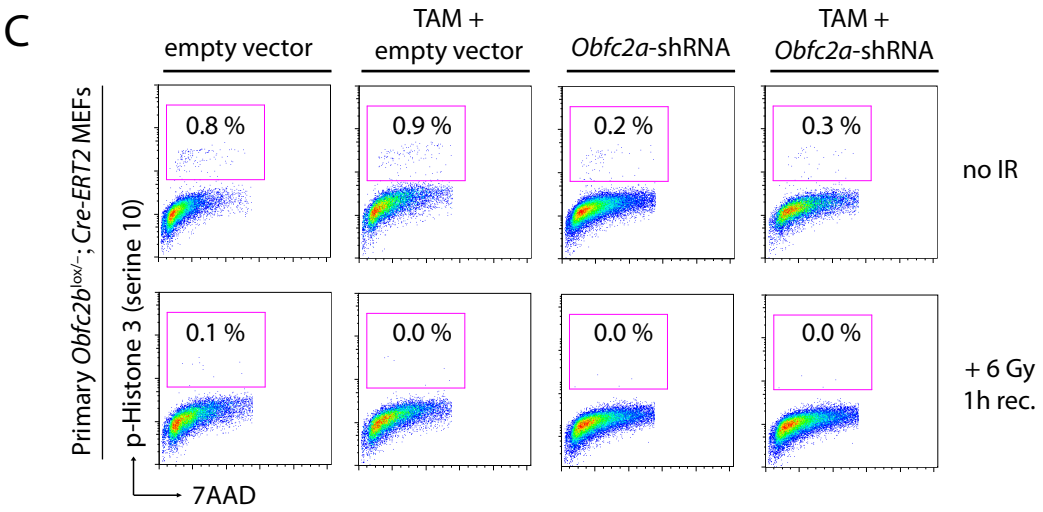

D

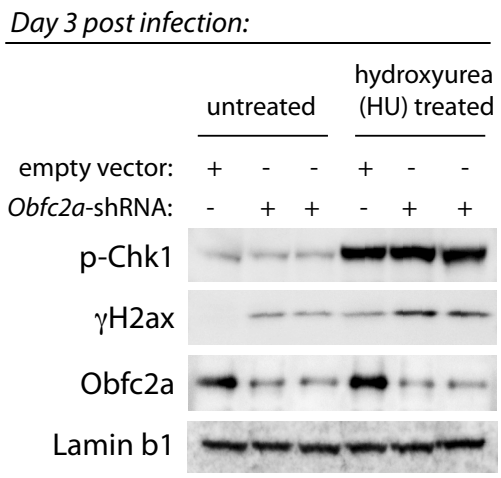

Supplemental Figure 7: Comparison of Obfc2b deficiency to Obfc2a and Obfc2b/Obfc2a double deficiency. (A,B,C) Analysis of SV40 transformed *Obfc2b*$^{lox/-}$*Cre-ERT2* MEFs infected with empty vector or *Obfc2a*-shRNA encoding vectors and treated with or without Tamoxifen (TAM) as described in Fig.7A. For TAM induced *Obfc2b* deletion, 2-3 days after infection MEFs were treated with 5μM TAM for 48 h. 3 days after TAM treatment MEFs were irradiated as indicated and harvested for analysis. Protein lysates from MEFs were analyzed by Western blot for Obfc2b, Obfc2a, phosphorylated H2ax (serine 139, γH2ax), Lamin b1, phosphorylated p53 (serine 15), phosphorylated Chk1 (serine 317) and phosphorylated Kap1 (serine 824). (B,C) Analysis of histone 3 phosphorylation (serine 10) by flow cytometry. Representative FACS plots are shown. Numbers indicate the percentage of cells exhibiting histone 3 phosphorylation. SV40-transformed (B) and primary (C) *Obfc2b*$^{lox/-}$*Cre-ERT2* MEFs as described in Figure 7A have been analyzed. (D) SV40 transformed *Obfc2b*$^{lox/-}$*Cre-ERT2* MEFs infected with empty vector or *Obfc2a*-shRNA encoding vectors were treated on day 3 post infection with 3mM hydroxyurea (HU) for 2 hours. MEFs were then analyzed by Western blot for Obfc2a, phosphorylated H2ax (serine 139, γH2ax), phosphorylated Chk1 (serine 317) and Lamin b1.